Local BLyS production by T follicular cells mediates retention of high affinity B cells during affinity maturation

Radhika Goenka,[1] Andrew H. Matthews,[1] Bochao Zhang,[2] Patrick J. O'Neill,[1] Jean L. Scholz,[1] Thi-Sau Migone,[3] Warren J. Leonard,[4] William Stohl,[5] Uri Hershberg,[2] and Michael P. Cancro[1]

[1]Department of Pathology and Laboratory Medicine, University of Pennsylvania, Philadelphia, PA 19104
[2]School of Biomedical Engineering, Science and Health Systems, Drexel University, Philadelphia, PA 19104
[3]Human Genome Sciences, Inc., Rockville, MD 20850
[4]Laboratory of Molecular Immunology, National Heart, Lung, and Blood Institute, Bethesda, MD 20892
[5]Division of Rheumatology, University of Southern California Keck School of Medicine, Los Angeles, CA 90033

We have assessed the role of B lymphocyte stimulator (BLyS) and its receptors in the germinal center (GC) reaction and affinity maturation. Despite ample BLyS retention on B cells in follicular (FO) regions, the GC microenvironment lacks substantial BLyS. This reflects IL-21–mediated down-regulation of the BLyS receptor TACI (transmembrane activator and calcium modulator and cyclophilin ligand interactor) on GC B cells, thus limiting their capacity for BLyS binding and retention. Within the GC, FO helper T cells (T_{FH} cells) provide a local source of BLyS. Whereas T cell–derived BLyS is dispensable for normal GC cellularity and somatic hypermutation, it is required for the efficient selection of high affinity GC B cell clones. These findings suggest that during affinity maturation, high affinity clones rely on T_{FH}-derived BLyS for their persistence.

CORRESPONDENCE
Michael P. Cancro:
cancro@mail.med.upenn.edu

Abbreviations used: AID, activation-induced deaminase; ASC, antibody-secreting cell; BAFF, B cell activating factor; Bcl6, B cell lymphoma 6; BCMA, B cell maturation antigen; BCR, B cell receptor; Blimp1, B lymphocyte–induced maturation protein 1; BLyS, B lymphocyte stimulator; BR3, BLyS receptor 3; CDR, complementarity determining region; CGG, chicken gamma globulin; DZ, dark zone; FDC, FO DC; FO, follicular; FWR, framework region; GC, germinal center; LZ, light zone; MFI, mean fluorescence intensity; NP, nitrophenacetyl; PNA, peanut agglutinin; SHM, somatic hypermutation; TACI, transmembrane activator and calcium modulator and cyclophilin ligand interactor.

The affinity maturation of antibodies involves competition among B cells expressing novel specificities generated by somatic hypermutation (SHM). This process occurs in germinal centers (GCs), transient structures formed during T cell–dependent immune responses that enable the preferential survival of B cells producing higher affinity antibodies. Ultimately, this competitive selection process preserves GC B cells with improved antigen affinity and eliminates those that lose specificity or gain autoreactivity. The mechanisms responsible for differential survival remain uncertain but involve tripartite interactions between the GC B cells, FO DCs (FDCs), and T FO helper (T_{FH}) cells. How the B cell receptor (BCR) drives this affinity-dependent selection process is debated. Although loss of BCR-associated signals disrupt GC kinetics (Wang and Carter, 2005; Huntington et al., 2006), recent findings suggest that antigen capture may be its primary function because BCR signaling is damped in most GC B cells by negative regulatory mechanisms (Khalil et al., 2012). This is consistent with models whereby GC B cells compete for antigen displayed on FDCs to mediate effective MHCII-restricted antigen presentation, thereby fostering sustained T_{FH} interactions, which in turn promote GC B cell survival (Allen and Cyster, 2008; McHeyzer-Williams et al., 2009; Victora and Nussenzweig, 2012). This idea is further supported by observations indicating that cognate T_{FH} interactions are a limiting factor in affinity maturation (Schwickert et al., 2011). Thus, higher affinity GC B cells can capture and present antigen more effectively, enabling their preferential access to T_{FH} cells and facilitating positive selection (Victora et al., 2010; Schwickert et al., 2011).

Despite mounting evidence for this model, the mechanism whereby T_{FH} interactions mediate selective survival of higher affinity GC B cells remains unclear. T–B interactions via receptors such as co-stimulatory molecules, death receptor ligands, and soluble survival factors are probably involved. However, the precise

© 2014 Goenka et al. This article is distributed under the terms of an Attribution–Noncommercial–Share Alike–No Mirror Sites license for the first six months after the publication date (see http://www.rupress.org/terms). After six months it is available under a Creative Commons License (Attribution–Noncommercial–Share Alike 3.0 Unported license, as described at http://creativecommons.org/licenses/by-nc-sa/3.0/).

The Rockefeller University Press $30.00
J. Exp. Med. 2014 Vol. 211 No. 1 45-56
www.jem.org/cgi/doi/10.1084/jem.20130505

The Journal of Experimental Medicine

Downloaded from http://rupress.org/jem/article-pdf/211/1/45/1749587/jem_20130505.pdf by guest on 09 February 2026

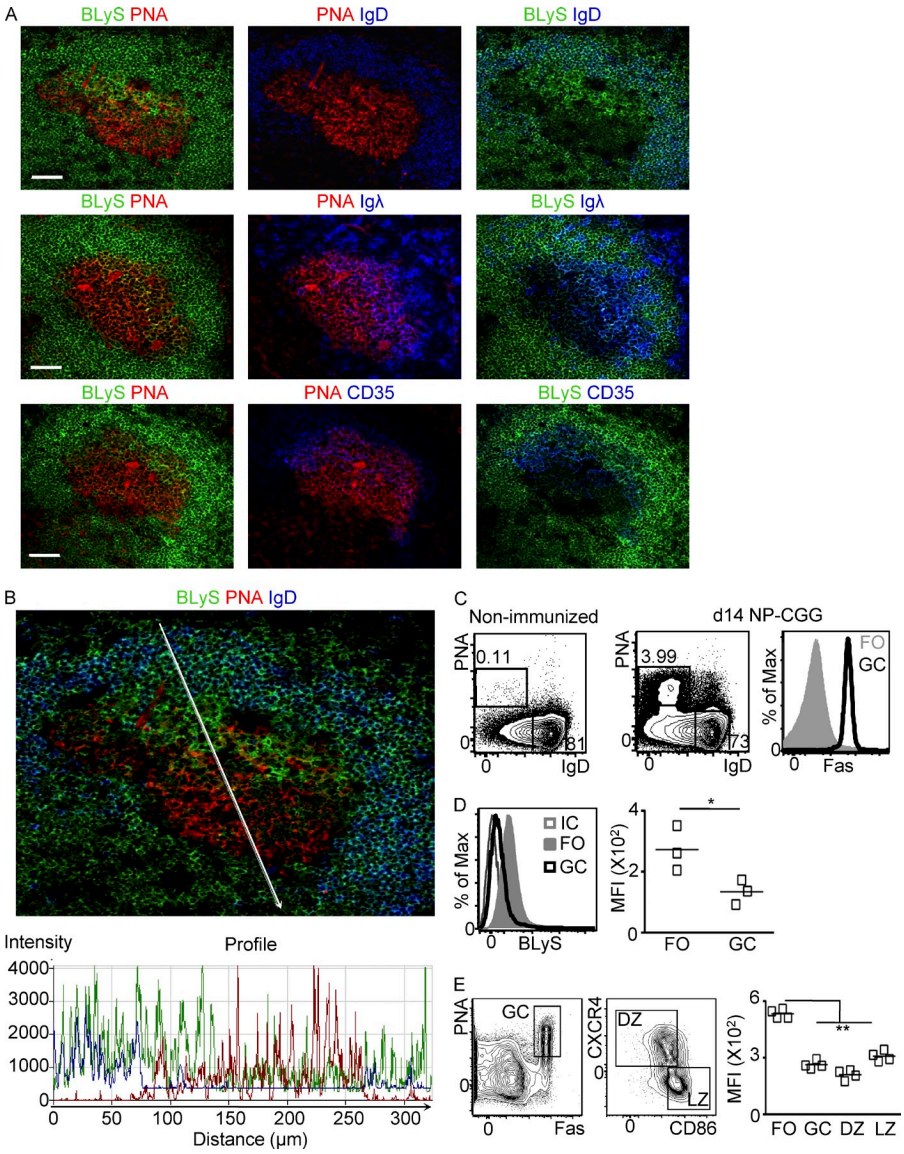

Figure 1. GCs are largely devoid of BLyS. (A) Mice were immunized with NP-CGG, and 14 d later spleen sections were stained with PNA and anti-BLyS antibody, as well as antibodies against IgD (top), Igλ (middle), or CD35 (bottom). Igλ-rich and CD35-rich regions demarcate the LZ and DZ, respectively. Bars, 50 µm. (B) Histogram analysis (bottom) of fluorescence pixel intensity of BLyS, PNA, and IgD staining through a cross section of a representative GC shown in A, top (from top to bottom along the white arrow). (C) Splenocytes from NP-CGG immunized mice were harvested at 14 d after immunization and stained with various antibodies against non–B and B lineage cells, as well as PNA to detect GC B cells. We gated on $CD4^-CD8^-F4/80^-Gr1^-CD19^+$ cells that were further subdivided into $PNA^+IgD^-Fas^{hi}$ GC B and $PNA^-IgD^+Fas^-$ FO B cells. (D) Splenocytes from NP-CGG immunized mice were harvested at 14 d after immunization and stained with anti-BLyS antibody or corresponding isotype control (IC) as well as other cell surface antigens to identify GC and FO B cells (outlined in C). Histogram overlays and MFI of BLyS bound to GC and FO B cell surfaces ($n = 3$ mice). Representative results are from more than three independent experiments. (E) Splenocytes were harvested at 14 d after immunization with NP-OVA. (Left) $CD4^-CD8^-F4/80^-Gr1^-CD19^+PNA^+IgD^-Fas^{hi}$ GC B cells (left histogram) were further subsetted into $CXCR4^{hi}CD86^{lo}$ DZ and $CXCR4^{lo}CD86^{hi}$ LZ (right histogram). (Right) BLyS expression on FO B and GC B as well as DZ and LZ GC B cells was assessed by flow cytometry using anti-BLyS antibody ($n = 4$ mice). Horizontal bars represent the mean of the points shown. * denotes statistical significance at $0.01 < P < 0.05$ and ** denotes statistical significance at $P < 0.01$ using a two-tailed Student's *t* test when compared with FO B cells.

identities and relative roles of these molecules remain obscure because most potential candidates also play roles in GC initiation or maintenance on their own. Therefore, separating these functions from direct roles in the preferential selection of high affinity clones has proven difficult. For example, the initiation and maintenance of GCs rely on sustained CD40/CD40L signals, and death receptors such as Fas/FasL interactions act to limit GC responses (Foy et al., 1993; Han et al., 1995; Hao et al., 2008). Similarly, soluble mediators such as IL-21 are essential for maintenance of GC B cell character as well as fate choices (Linterman et al., 2010; Zotos et al., 2010).

The B lineage survival cytokine, B lymphocyte stimulator (BLyS, also termed B cell activating factor [BAFF]), plays a key role in setting thresholds for BCR-mediated selection among naive B cells (Cancro, 2004), making it an attractive candidate for mediating analogous processes in the GC. Consistent with this notion, GC responses prematurely terminate in mice with either global BLyS deficiency or defects in BLyS receptor 3 (BR3, also known as BAFFR) signaling (Rahman et al., 2003). Straightforward interpretation of these findings is difficult, because both BLyS-deficient and BR3 mutant mice are severely B lymphopenic (Moore et al., 1999; Schneider et al., 1999; Yan et al., 2001a). Thus, deficits in naive B cell numbers might explain an inability to sustain GC reactions because GCs are resupplied from the naive pools (Schwickert et al., 2007). Moreover, defects in FDC network maturation and T_{FH} function also occur in B lymphopenic environments (Rahman et al., 2003; Johnston et al., 2009). Thus, whether BLyS plays a direct role in GC B cell selection and affinity maturation has remained unclear.

Downloaded from http://rupress.org/jem/article-pdf/211/1/45/1749587/jem_20130505.pdf by guest on 09 February 2026

To better understand how BLyS influences GC function, we investigated the distribution and expression of BLyS and its receptors during GC responses in normal mice. We find that BLyS is spatially segregated between the follicles and GCs, as well as within the GCs, where it is found mainly in the light zone (LZ). Thus, in contrast to FO B cells, GC B cells lack appreciable surface-bound BLyS. This results from profound down-regulation of the BLyS receptor, transmembrane activator and calcium modulator and cyclophilin ligand interactor (TACI), which occurs as FO B cells adopt GC B character after IL-21 signals in the context of BCR cross-linking and CD40 co-stimulation. However, in the LZ BLyS is highly expressed by and associated with FO T cells, both helper (T_{FH}) and regulatory (T_{FR}). Mixed BM chimeras that lack T cell–derived BLyS have normal GC cellularity and low-affinity IgM and IgG1 antibodies but exhibit significant reductions in high affinity antibody. Moreover, although SHM occurs under these conditions, the patterns of mutation are broadly distributed and show a lower strength of positive selection. Together, these findings indicate that T_{FH}-derived BLyS is required to preserve high affinity clones among antigen binding GC B cells.

RESULTS

GC B cells lack receptor-bound BLyS

Neither BLyS distribution nor BLyS receptor expression within GCs has been extensively examined in situ. Accordingly, we used confocal fluorescence microscopy and flow cytometry to assess these parameters in splenic GCs 14 d after immunization with the nitrophenacetyl (NP) hapten conjugated to chicken gamma globulin (NP-CGG). Consistent with prior studies indicating that the BLyS binding capacity of FO B cells is nearly saturated under steady-state conditions in vivo (Lesley et al., 2004), cells in the peanut agglutinin (PNA) IgD^+ FO regions were consistently decorated with BLyS (Fig. 1, A and B). In contrast, PNA^+IgD^- GC B cells displayed minimal BLyS staining. Indeed, little if any BLyS was visible in the GC dark zone (DZ), and only a fine network of staining was seen in the $Ig\lambda^+$ or $CD35^+$ LZ (Fig. 1 A). This distribution was confirmed by quantitative analyses of staining intensity through GC cross sections, where the green pixels corresponding to BLyS positivity had higher intensity in the IgD-rich FO regions compared with a majority of the PNA-rich GC areas (Fig. 1 B).

Because most systemic BLyS is bound to receptors on B cell surfaces in vivo (Lesley et al., 2004), we used flow cytometry to determine the relative amounts of BLyS present on the surface on FO B versus GC B cells immediately ex vivo. We stained splenocytes harvested at day 14 after immunization with anti-BLyS antibody and determined the mean fluorescence intensity (MFI) of BLyS on FO B and GC B cells (Fig. 1, C–E). Consistent with our histological observations, this analysis revealed that GC B cells are uniform in terms of surface-bound BLyS and, as indicated by twofold lower MFI, have less bound BLyS than FO B cells; within the GC, both LZ and DZ B cells bind less BLyS than FO B cells (Fig. 1 E).

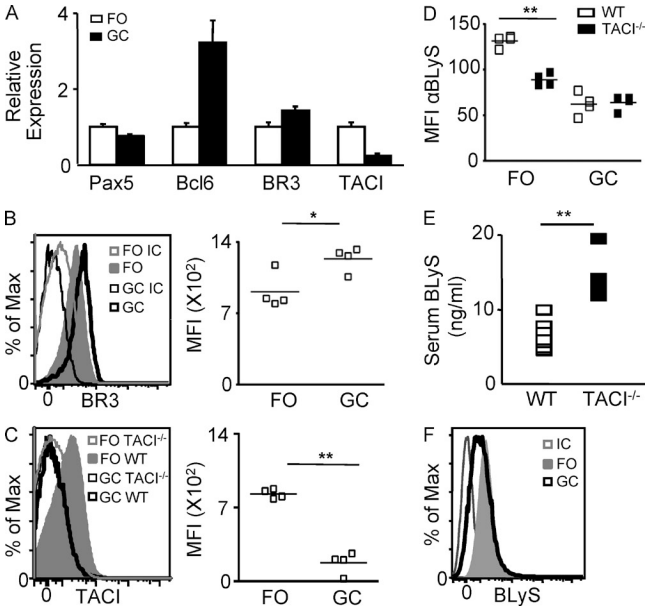

Figure 2. TACI mediates partitioning of BLyS between FO and GC B cells. WT (A–D) or $TACI^{-/-}$ (C, D, and F) mice were immunized with NP-CGG and splenocytes were harvested at day 14. (A) GC and FO B cells from WT mice were FACS sorted and expression of TACI, BR3, Bcl6, and Pax5 was assessed by qPCR and normalized to FO B cells. Representative results are from five independent experiments. Error bars represent ±1 SD. (B and C) Expression of BR3 (B) and TACI (C) was assessed on GC B and FO B cells in WT mice (IC = isotype control). In C, cells from $TACI^{-/-}$ mice were used as a control. Representative results from three independent experiments. (D) MFI of BLyS bound to FO B or GC B cells in WT or $TACI^{-/-}$ mice (n = 4 mice). Horizontal bars in B–D represent the mean of the points shown. (E) BLyS concentrations were measured in sera of WT (n = 14) or $TACI^{-/-}$ (n = 7) mice by ELISA. (F) BLyS expression on FO B and GC B cells present in $TACI^{-/-}$ mice was assessed by flow cytometry using anti-BLyS antibody (IC = isotype control). Representative results are from more than two independent experiments with n = 3–4 mice per experiment. * denotes statistical significance at $0.01 < P < 0.05$ and ** denotes statistical significance at $P < 0.01$ using a two-tailed Student's t test.

Because most systemic BLyS is secreted as free trimers (Mackay and Schneider, 2009), and there are no physical barriers between the follicle and the GC, we reasoned that the disparity in bound BLyS likely reflects changes in the expression or proportions of BLyS receptors on GC versus FO B cells. We therefore analyzed the expression of all three BLyS receptors on GC B and FO B cells by both qPCR and FACS (gating shown in Fig. 1 C). As expected, GC B cells were enriched for the transcription factor B cell lymphoma 6 (Bcl6) and maintained Pax5 expression when compared with FO B cells (Fig. 2 A; Shaffer et al., 2002). In accord with prior studies, FO B cells express both BR3 and TACI (Hsu et al., 2002; O'Connor et al., 2004; Stadanlick et al., 2008). In contrast, although GC B cells continue to express BR3 message and protein (Fig. 2, A and B), TACI expression is profoundly down-regulated (Fig. 2, A and C). Interestingly, BR3 surface levels assessed by MFI are slightly higher on GC B cells than on FO B cells, despite similar message levels. The basis for this

Downloaded from http://rupress.org/jem/article-pdf/211/1/45/1749587/jem_20130505.pdf by guest on 09 February 2026

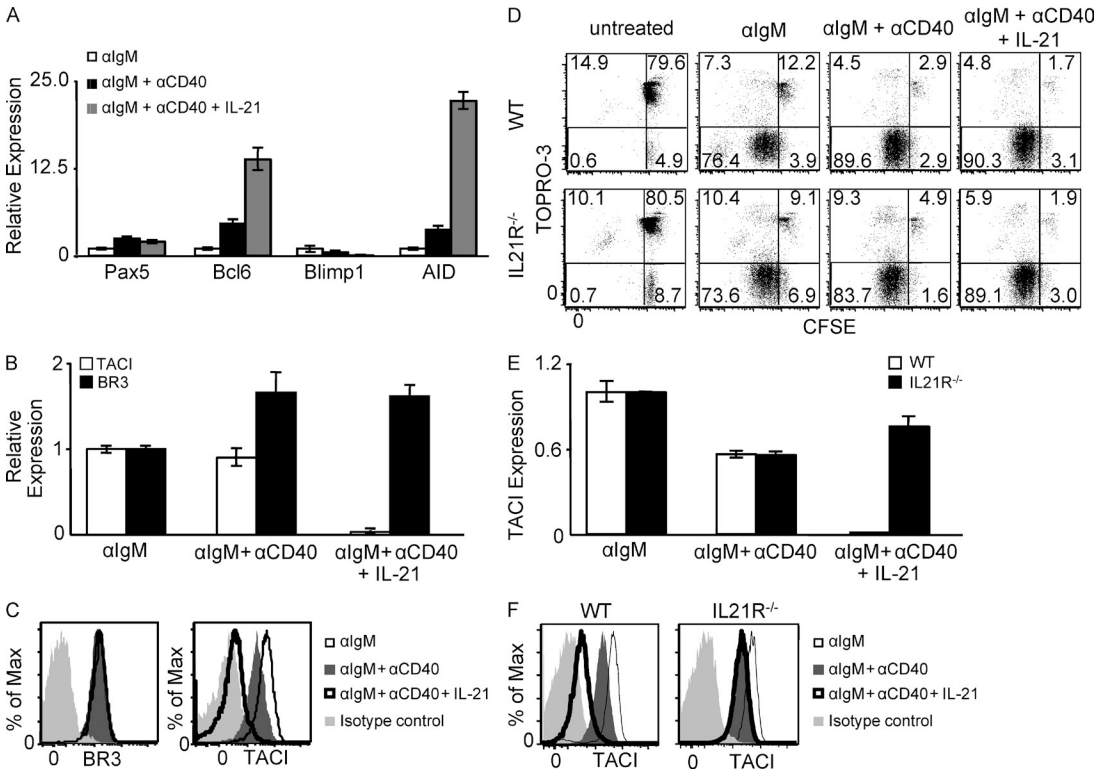

Figure 3. IL-21 induces TACI down-regulation in activated B cells. (A–C) CD23$^+$ splenocytes from WT mice were stimulated with F(ab)′$_2$ αIgM alone or in combination with αCD40 with or without IL-21 for 3 d. Representative results are from more than three independent experiments. (A) Expression of Pax5, Bcl6, Blimp1, and AID were assessed by qPCR. (B and C) Cells were stimulated as described in A, and expression of TACI and BR3 was assessed by qPCR (B) or flow cytometry (C). In B, expression is normalized to αIgM-stimulated cells. (D–F) CD23$^+$ splenocytes from WT or IL-21R$^{-/-}$ mice were stimulated with F(ab)′$_2$ αIgM alone or in combination with αCD40 with or without IL-21 for 3 d. Representative results are from two independent experiments. (D) Proliferation and viability profiles for the cultures shown in E and F were assessed by dilution of CFSE and exclusion of TOPRO-3, respectively. (E and F) Expression of TACI was assessed by qPCR (E) or flow cytometry (F). In E, expression is normalized to αIgM-stimulated cells. Error bars represent ±1 SD.

is unclear but may reflect altered surface turnover or recycling. Neither FO nor GC B cells express B cell maturation antigen (BCMA; unpublished data).

The paucity of bound BLyS on GC B cells correlates with TACI down-regulation, suggesting that TACI is responsible for most retained BLyS on FO B cells, and that TACI down-regulation yields the disparate distribution of BLyS between follicles and GCs. These possibilities were investigated through ex vivo staining of FO and GC B cells from control WT and TACI-deficient mice (Mantchev et al., 2007). Our analyses revealed that TACI-deficient FO B cells have less surface-bound BLyS than FO B cells from WT mice (Fig. 2 D). Consistent with this reduction in FO B cell BLyS binding capacity, TACI-deficient mice had significantly higher levels of free serum BLyS than did WT mice (Fig. 2 E; Bossen et al., 2008). Importantly, TACI deficiency eliminated the difference in surface-bound BLyS between GC and FO B cells (Fig. 2, D and F). Therefore, TACI is critical for the retention of BLyS on FO B cells, suggesting that the disparate TACI receptor density between FO B and GC B cells is necessary to partition systemic BLyS into the FO regions and out of GCs, yielding BLyS-rich and BLyS-poor microenvironments, respectively. Moreover, because much less bound BLyS is retained on GC B cells owing to the loss of TACI, overall BLyS binding may be less avid, yielding less frequent or sustained BR3 occupation.

IL-21 extinguishes TACI expression in activated B cells

The negligible TACI expression among GC B cells prompted us to ask whether stimuli that foster a GC B cell transcriptional profile regulate TACI expression. Enriched FO B cells were stimulated for 3 d with combinations of F(ab′)$_2$ anti-Ig, anti-CD40, and IL-21, a GC fate-promoting cytokine (Linterman et al., 2010; Zotos et al., 2010). As previously reported, in the context of BCR and CD40 ligation, IL-21 engenders GC character by up-regulating Bcl6 and activation-induced deaminase (AID), maintaining Pax5, and down-regulating B lymphocyte–induced maturation protein 1 (Blimp1; Fig. 3 A; Goenka et al., 2011). Although BCR and CD40 ligation modestly down-regulate surface TACI levels, TACI mRNA is not affected (Fig. 3, B and C). In contrast, the addition of IL-21 under these conditions fully extinguishes TACI, but not BR3, expression (Fig. 3, B and C). Addition of other cytokines, such as IL-4 or IL-6, did not alter TACI expression (unpublished data). To confirm that IL-21/IL-21R

Downloaded from http://rupress.org/jem/article-pdf/211/1/45/1749587/jem_20130505.pdf by guest on 09 February 2026

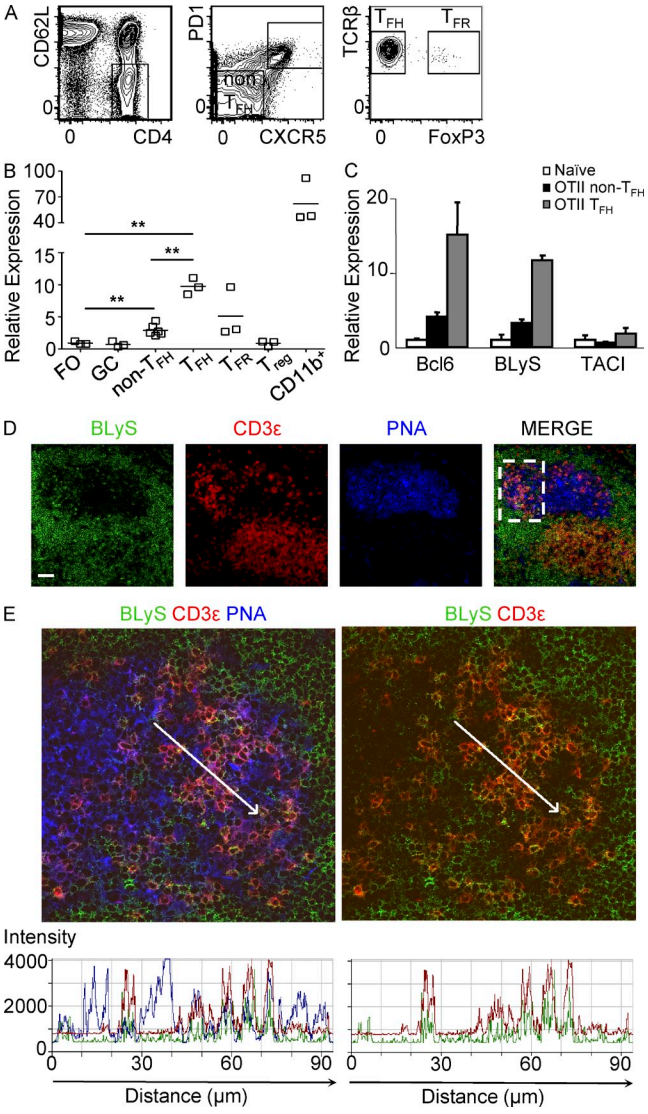

Figure 4. T_{FH} and T_{FR} cells produce BLyS in the GC. (A and B) FoxP3-eGFP knockin mice were immunized with NP-OVA and splenocytes were isolated at day 7 after immunization. (A) $B220^-TCR\text{-}\beta^+CD4^+CD62L^-$ cells were gated and further subsetted into non-T_{FH} ($PD1^-CXCR5^-$), T_{FH} ($PD1^+CXCR5^+FoxP3^-$), or T_{FR} ($PD1^+CXCR5^+FoxP3^+$). Gating strategy for $B220^-TCR\text{-}\beta^+CD4^+CD62L^+FoxP3^+$ (T_{reg} cells) is not shown. Representative results are from more than two independent experiments. (B) $CD11b^+$ myeloid (positive control), FO B, GC B, non-T_{FH}, T_{FH}, T_{FR}, and T_{reg} cells were FACS sorted and BLyS expression was measured by qPCR. Expression was normalized to FO B cells ($n > 3$ mice). Horizontal bars represent the mean of the points shown. (C) $CD45.2^+$ OVA-specific OTII T cells were transferred into B6.SJL ($CD45.1^+$) mice and the hosts mice were immunized with NP-OVA. After 10 d, splenic naive endogenous CD4 T cells ($CD45.2^-CD62L^+CXCR5^-$), as well as ova-specific non-T_{FH} ($CD45.2^+CD62L^-PD1^-CXCR5^-$) and T_{FH} ($CD45.2^+CD62L^-PD1^+CXCR5^+$) cells, were FACS sorted, and Bcl6, BLyS, and TACI expression was measured by qPCR. Expression was normalized to naive T cells. Data are presented as mean ± SD and representative of more than two independent experiments. (D and E) WT mice were immunized with NP-CGG, and 14 d later spleen sections were stained with PNA, anti-BLyS, and anti-CD3ε antibodies. Bar, 50 μm. (E) Histogram analysis (bottom) of fluorescence pixel intensity of BLyS, PNA, and CD3ε along the white arrow drawn across a cross section of the GC shown in D (dashed box). Representative results are from more than three independent experiments.

signaling abrogates TACI expression, we repeated the experiment with IL-21R–deficient cells. Activated WT and IL-21R$^{-/-}$ cells had comparable viability and proliferation profiles as assessed by exclusion of TOPRO-3 and by dilution of CFSE, respectively (Fig. 3 D). As expected, IL-21–mediated TACI down-regulation was not observed in IL-21R–deficient B cells (Fig. 3, E and F). Thus, TACI down-regulation is a fundamental component of the overall GC B cell transcriptional profile induced by IL-21 signals received in the context of BCR and CD40 ligation.

T_{FH} cells are a local BLyS source in the GC

Because our flow cytometric analyses revealed that GC B cells have uniformly less BLyS bound to their surface and lack TACI (Fig. 1, D and E; Fig. 2 C), we reasoned that $BLyS^+$ cells in the GC LZ are unlikely to be a subset of GC B cells that retain robust BLyS binding capacity. Instead, BLyS might be produced by other GC resident cells such as FDCs, T_{FH} cells, or T_{FR} cells (Hase et al., 2004; Chung et al., 2011; Linterman et al., 2011). Accordingly, we evaluated the BLyS expression among GC B, T_{FH}, and T_{FR} cells. Each of these cell populations, as well as naive FO B cells, were sorted from FoxP3-eGFP knockin mice at day 7 after immunization with NP-OVA, according to the gating strategy shown in Fig. 4 A. GC B cells expressed little if any BLyS, whereas both T_{FH} and T_{FR} cells were enriched for BLyS transcripts (Fig. 4 B). To determine if FO T lineage cells were unique in their ability to produce BLyS, we measured BLyS transcripts in non-T_{FH} effector and regulatory T cells (T_{reg} cells). We find that although non-T_{FH} cells produce BLyS, albeit at lower levels than FO T cells, T_{reg} cells do not express BLyS (Fig. 4 B). To more precisely track BLyS expression by T_{FH} cells in an ongoing immune response, we transferred $CD45.2^+$ OVA-specific OTII T cells into B6.SJL ($CD45.1^+$) hosts. At 10 d after NP-OVA immunization, we sorted the OTII-derived T_{FH} cells and found that they expressed ∼10-fold higher levels of BLyS transcripts than did naive $CD4^+$ T cells (Fig. 4 C). Moreover, although some T cell subsets express TACI (von Bülow and Bram, 1997), OVA-specific T_{FH} cells did not (Fig. 4 C), arguing against the possibility that T_{FH} sequester BLyS in the LZ through TACI.

To confirm that BLyS protein is made by GC-resident T cells, we performed immunohistological analyses on spleens from mice at day 14 after NP-CGG immunization. CD3ε positivity (red) colocalized with $BLyS^+$ pixels (green) in the GC, and thus appeared yellow in the merged image (Fig. 4, D and E). The boxed cross section of the GC shown in Fig. 4 D was imaged at a higher magnification and shown in Fig. 4 E. Pixel intensity was determined along the white arrow (from left to right, Fig. 4 E) and depicted as a histogram. Intense BLyS staining is largely congruent with CD3ε in the GC

Downloaded from http://rupress.org/jem/article-pdf/211/1/45/1749587/jem_20130505.pdf by guest on 09 February 2026

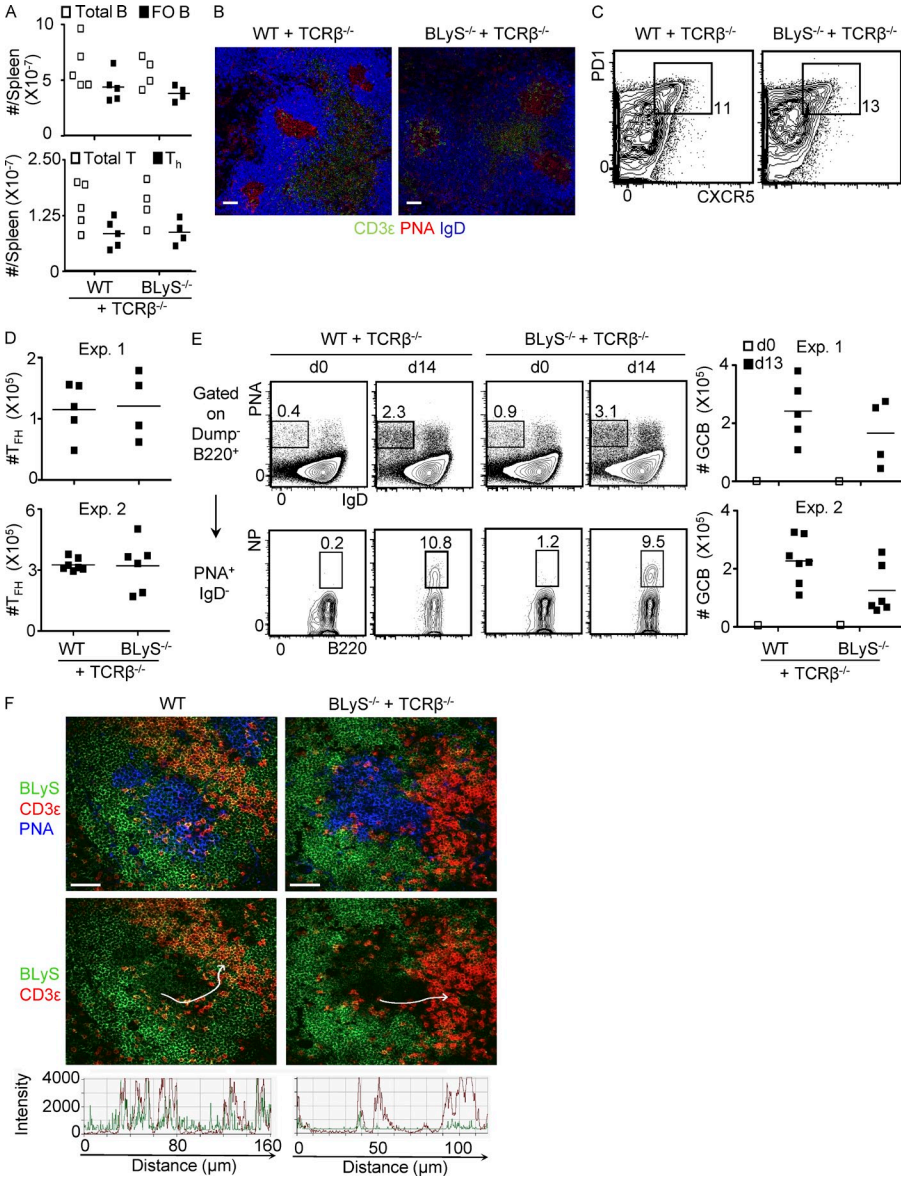

Figure 5. Normal development of GCs in the absence of BLyS produced by T cells. Mixed BM chimeras were generated by mixing BM (depleted of $CD3^+$, $Gr1^+$, and $B220^+$ cells) from TCR-$\beta^{-/-}$, BLyS$^{-/-}$, or WT mice in a ratio of 25:75 TCR-$\beta^{-/-}$/BLyS$^{-/-}$ or 25:75 TCR-$\beta^{-/-}$/WT. The cells were injected i.v. into lethally irradiated WT mice. The mice were allowed to reconstitute for ≥11 wk, and then immunized with NP-CGG. Spleens were harvested 13 d later. All results derive from two independent experiments. (A) Numbers of $B220^+$ (total B) and $B220^+IgD^{hi}$ FO B cells (left), as well as TCR-β^+ (total T) and $CD4^+$TCR-β^+ T_H cells (right) per spleen for the indicated chimeras ($n = 5$). (B) GC architecture was analyzed using PNA and antibodies against IgD and CD3ε. Bar, 50 μm. (C) Representative gating strategy to identify T_{FH} cells as $B220^-$TCR-$\beta^+CD4^+CD62L^-CXCR5^+PD1^+$ cells. (D) Number of T_{FH} cells per spleen of immunized mice ($n > 4$). (E, left) Representative gating strategy to identify GC B cells as dump$^-$ ($CD4^-CD8^-F4/80^-Gr1^-$) $B220^+IgD^-PNA^+NP^+$. (E, right) Number of NP^+ GC B cells per spleen of immunized mice ($n \geq 4$). (F) Confocal micrographs of spleen sections stained with PNA, anti-BLyS, and anti-CD3ε antibodies (top), along with histogram analysis of fluorescence pixel intensity of BLyS and CD3ε along the white arrow drawn across the cross section of the GC (bottom). Bar, 50 μm.

(Fig. 4 E, right) and not with PNA (Fig. 4 E, left). Thus, BLyS in the GC LZ is primarily attributed to T cells, the majority of which are T_{FH} cells (Chung et al., 2011; Linterman et al., 2011).

T cell–restricted BLyS deficiency yields normal GC formation but impairs affinity maturation

These findings indicated that FO T cells are a local source of BLyS within the otherwise BLyS-poor GC microenvironment and, coupled with continued BR3 expression but low BLyS retention capacity by GC B cells, led us to ask whether T cell–derived BLyS is important for GC initiation, maintenance, or selection. By reconstituting lethally irradiated hosts with TCR-$\beta^{-/-}$ BM combined with either BLyS$^{-/-}$ or WT BM, we generated mixed BM radiation chimeras in which the T lineage lacks BLyS. Importantly, systemic BLyS levels are unperturbed in such chimeras because hematopoietic sources of BLyS contribute minimally to systemic BLyS production or to the establishment and maintenance of primary B cell pools (Gorelik et al., 2003). Thus, reconstitution of the primary B cell pools in WT and BLyS$^{-/-}$ chimeras was comparable, achieving normal steady-state numbers by 11 wk after BM transfer (Fig. 5 A). Furthermore, naive T cells numbers were also normal and similar in both types of chimeras (Fig. 5 A). Finally, in BLyS$^{-/-}$ T cell chimeras, FDCs should be BLyS-sufficient because they are radioresistant and originate from nonhematopoietic precursors (Kapasi et al., 1998; Krautler et al., 2012), making T_{FR} and T_{FH} the only BLyS-producing, GC-resident cells that lack BLyS. Although some myeloid cells may also be derived from the BLyS-deficient donor, they are not known to influence GC B cells directly (Grouard et al., 1996); moreover, T_{FR} cells likely do not interact directly with GC B cells (Sage et al., 2013).

Once full reconstitution was achieved, the chimeras were immunized with NP-CGG. At 2 wk after immunization,

Downloaded from http://rupress.org/jem/article-pdf/211/1/45/1749587/jem_20130505.pdf by guest on 09 February 2026

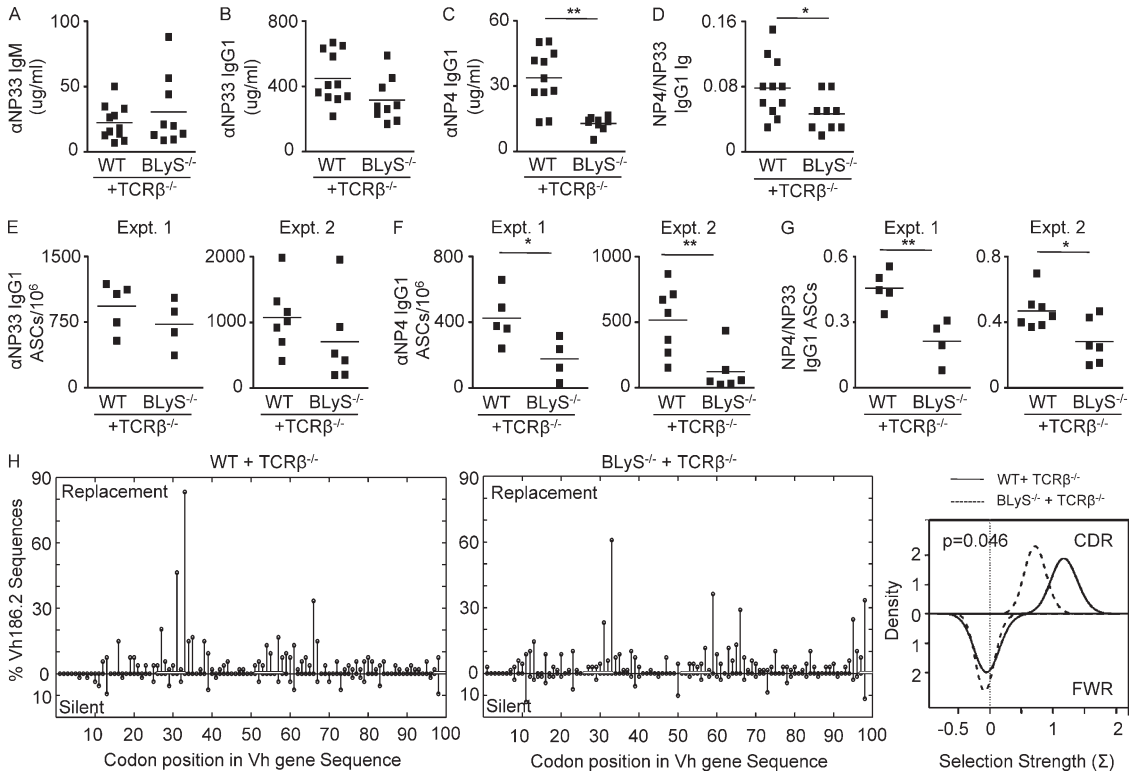

Figure 6. Reduced positive selection and high-affinity antibody production in the absence of T cell–derived BLyS. (A–F) Mixed BM chimeras were generated as described in Fig. 5 and immunized with NP-CGG. After 13 d, NP-specific serum Igs, as well as splenic ASCs, were analyzed using ELISA or ELISpot, respectively. We used NP33-BSA– or NP4-BSA–coated plates to determine total or high affinity Ig/ASCs, respectively. (A–D) The concentration of total NP-specific IgM (A) or IgG1 (B) and high-affinity IgG1 (C), as well as the ratio of high affinity/total IgG1 serum Ig (D; $n > 9$). Data are derived from sera samples that were obtained from two experiments. (E–G) Number of NP-specific total (E) and high affinity (F) IgG1 splenic ASCs, as well as the ratio of high affinity/total IgG1 ASCs (G) in the chimeras ($n > 4$ mice). Results from two independent experiments are shown. Horizontal bars in A–G represent the mean of the points shown. (H–I) Chimeras were immunized with NP-CGG, and after 15 d, 2,000 GC B cells were FACS sorted. Vh186.2$^+$ gene was amplified using RT-PCR, and the amplicon was cloned and sequenced. Data are derived from sequences (WT, 54; BLyS$^{-/-}$ T, 69) that were obtained from two experiments. (H) Depiction of replacement or silent mutations at specific codons in the Vh186.2 sequence in WT or BLyS$^{-/-}$ T chimeras. Numbers above and below the line indicate the occurrence of replacement and silent mutations in a specific codon, respectively. CDR1 and 2 and the three first codons of CDR3 are marked with a thick black line. Total numbers of mutations are normalized to the total number of sequences. (I) Sequences were subjected to the BASELINe mutation analysis software in which positive values of selection strength indicate positive selection and negative values indicate negative selection. Curves above the line measure selection strength in CDR and below the line in FWR. The p-value in the top left corner is of the comparison of selection strength in the CDRs of WT and BLyS$^{-/-}$ T chimeras mice. * denotes statistical significance at $0.01 < P < 0.05$ and ** denotes statistical significance at $P < 0.01$ using a two-tailed Student's *t* test.

GC formation and architecture were intact in both groups of chimeric mice; GCs formed near the T-B border and were similar in size (Fig. 5 B). Similarly, key GC architectural features were preserved because LZs were populated with T cells (Fig. 5, B and F), and the numbers of PD1^{hi}CXCR5$^+$ GC T_{FH} cells did not significantly differ between the chimeras (Fig. 5, C and D). When compared with control chimeras, there was a modest but consistent (~1.5-fold) reduction in NP-specific GC B cells in BLyS-deficient T cell chimeras, but this did not achieve statistical significance (Fig. 5 E). Importantly, immunohistochemistry confirmed that BLyS co-localized with GC LZ T cells in WT control but not BLyS$^{-/-}$ T cell chimeras (Fig. 5 F), thus substantiating the origin of T cells in each chimera type, and further confirming the specificity of BLyS staining in histological sections. Moreover, T_{FH} cells appear to be a major source of BLyS within the GC, as the disparity in BLyS distribution between LZ and DZ was minimal in the BLyS$^{-/-}$ T chimeric mice (Fig. 5 F).

Having established that GC initiation, magnitude, and composition were largely normal in these chimeras, we measured NP-reactive antibody-secreting cells (ASCs) and serum antibody in these mice to investigate whether the absence of T_{FH}-derived BLyS affects affinity maturation. Analysis on highly substituted NP conjugates revealed that both types of chimeric mice had comparable serum levels of total NP-specific IgM (Fig. 6 A) and IgG1 antibody (Fig. 6 B), as well as similar numbers of total NP-specific IgG1 ASCs (Fig. 6 E). However, despite antibody and ASC responses of similar magnitude and isotype composition, the BLyS$^{-/-}$ T cell chimeras had significant reductions in both IgG1 high affinity antibody (Fig. 6 C) and ASCs (Fig. 6 F). Moreover, the ratio of high affinity to total antibody (Fig. 6 D) as well as ASCs (Fig. 6 G) was also

Downloaded from http://rupress.org/jem/article-pdf/211/1/45/1749587/jem_20130505.pdf by guest on 09 February 2026

Table 1. Summary of somatic mutations observed in the Vh186.2 sequences from GC B cells

Chimera type	*n*	FWR (1+2+3)		CDR (1+2)	
		# R	# S	#R	#S
WT + TCR-β$^{-/-}$	54	2.69 ± 1.78	0.98 ± 1.04	2.31 ± 1.24	0.31 ± 0.46
BLyS$^{-/-}$ + TCR-β$^{-/-}$	69	3.17 ± 1.57	1.22 ± 1.16	1.81 ± 1.06	0.51 ± 0.63

GC B cells (Dump$^-$B220$^+$PNA$^+$Fas^{hi}NP$^+$) were FACS sorted at day 15 after immunization with NP-CGG. Sequences were pooled from two independent experiments. In each experiment, we sorted 2,000 NP$^+$ GC B cells from splenocytes pooled from three WT and three BLyS$^{-/-}$ T cell chimeras. R denotes replacement and S denotes silent mutations. FWR and CDR values represent mean ± SD.

reduced when T cells were unable to synthesize BLyS. Thus, T_{FH}-derived BLyS is dispensable for early antibody responses, for GCs of normal structure and magnitude, and for ASC differentiation but is required for normal affinity maturation.

Impaired affinity maturation reflects a failure of focused selection among somatically mutated GC B cells

The failure to achieve normal levels and proportions of high affinity ASCs and serum antibody might reflect either a defect in the initiation or extent of somatic mutation on its own, or a failure to preserve high affinity clones at the expense of those with spurious or detrimental mutations. To investigate these possibilities, we sequenced heavy chains of sorted NP-specific GC B cells from each chimera and performed three analyses to assess the numbers and pattern of mutations, as well as the presence and strength of positive and negative selection in the framework regions (FWRs) and complementarity determining regions (CDRs).

The pattern of mutations was clearly different between control and experimental chimeric mice. The W33L replacement was present in GC B cells from both chimeras, albeit at reduced frequency in BLyS$^{-/-}$ T cell chimeras than the control chimeras (Fig. 6 H). However, GC B cells in control chimeras exhibited a restricted pattern of replacement (R) mutations (Fig. 6 H), whereas GC B cells in BLyS$^{-/-}$ T cell chimeras displayed a more broadly distributed pattern of R mutations, with a reduced preference for W33L, and many additional R and S mutations (Fig. 6 H). Furthermore, the R to S ratio in the CDR of WT chimera was much higher than in the BLyS$^{-/-}$ T chimera (∼8 vs. ∼3.5, Table 1). Because altered mutation patterns can influence specificity-based selection, we applied the focused binomial test to determine whether selection was occurring comparably among the GC B cells of these mice (Hershberg et al., 2008; Uduman et al., 2011). This test affords greater specificity in detecting selection than previous R/S ratio methods because it more precisely accounts for inherent biases of somatic mutation through comparisons of the number and distribution of R mutations in areas of interest (CDR or FWR) to the total level of S mutations in the entire sequence. Results from this test revealed that GC B cells from neither the WT nor the BLyS$^{-/-}$ T cell chimeras displayed selection in the FWR, whereas both had significant positive selection in the CDR ($P < 0.05$).

Finally, to quantify selection strength we used BASELINe, which yields a full probability distribution of estimated selection strength (Uduman et al., 2011; Yaari et al., 2012). This analysis revealed that both chimeras preserved the FWR, thus indicating similar and negligible levels of negative selection against changes in their FWR regions (Fig. 6 I). In contrast, although antigen-specific GC B cells from both chimeras exhibited positive selection within CDRs, the strength of positive selection in the CDRs of WT chimeras was significantly stronger than in BLyS$^{-/-}$ T cell chimeras ($P < 0.05$ and Fig. 6 I). In conjunction with the selective loss of high affinity ASCs and antibody in BLyS$^{-/-}$ T cell chimeras, these findings suggest that T_{FH}-derived BLyS is required to promote and maintain GC B cells that achieve high affinity.

DISCUSSION

In this study, we examined how BLyS and its receptors influence the GC reaction. The results reveal that BLyS is spatially segregated both at the GC–follicle interface and within GCs themselves. BLyS partitioning between the GC and follicle relies on differential BLyS receptor densities in these regions, which is afforded by IL-21–driven TACI down-regulation in stimulated B cells. Within the GC, BLyS is localized in the LZ, reflecting production by T_{FH}/T_{FR} cells. Furthermore, results from mixed BM chimeras reveal that although T cell–elaborated BLyS is dispensable for GC initiation and the generation of normal T_{FH} and GC B cell numbers, it is required for the persistence of high-affinity GC B cells. Based on these findings, we propose a model whereby B–T cell interactions govern BLyS availability within the GC, allowing cells that have acquired high affinity to survive.

The striking anatomical sequestration of BLyS reveals a mechanism for restricting BLyS availability without physical barriers. Based on several observations, we favor the notion that TACI down-regulation on its own is responsible for partitioning BLyS between the FO and GC regions. First, in normal mice, the BLyS binding capacities of FO and GC B cells directly correspond to TACI expression (Fig. 2). Second, TACI-deficient mice exhibit uniformly low levels of bound BLyS on their FO and GC B cells, display corresponding increases in free serum BLyS (Fig. 2), and fail to generate strongly demarcated BLyS-rich and BLyS-poor FO and GC regions after immunization. This relationship between BLyS retention and TACI expression effectively sequesters systemic BLyS in the follicles, and enables the creation of BLyS-poor

Downloaded from http://rupress.org/jem/article-pdf/211/1/45/1749587/jem_20130505.pdf by guest on 09 February 2026

microenvironments where locally generated BLyS can be leveraged as a selecting agent. This model predicts that an inability to create BLyS-poor microenvironments through this mechanism would thwart competitive selection, yield protracted GC kinetics, and impair the generation of high affinity ASCs. Indeed, despite enlarged and persistent GCs in TACI-deficient mice, the BM ASC pool is reduced (Yan et al., 2001b; Seshasayee et al., 2003; Tsuji et al., 2011; not depicted). Finally, our findings also suggest that TACI, although not required for FO B cell survival, is critical for retaining BLyS on FO B cell surfaces. This may reflect efficient binding of higher order BLyS multimers to TACI, as well as increased avidity afforded by two ligand-binding domains in the TACI trimer compared with only a single, partial binding domain in BR3 (von Bülow and Bram, 1997; Thompson et al., 2001; Bossen et al., 2008).

Because T_{FR} cells do not produce IL-21 and are not thought to interact directly with GC B cells (Linterman et al., 2011; Sage et al., 2013), we propose that T_{FH} cells orchestrate conditions that foster local BLyS availability in the GC through a bilateral mechanism. First, IL-21 mediates TACI down-regulation on GC B cells, so sustained IL-21 signals will not only maintain GCs but also limit the intrinsic BLyS binding ability of GC B cells. Although this scenario awaits in vivo confirmation, it is consistent with the inability of IL21R-deficient mice to maintain GCs, and suggests that the failure to enforce TACI down-regulation and other aspects of GC B cell character might underlie aspects of this phenotype. Second, T cells are the predominant source of BLyS in GCs because T_{FH} and T_{FR}, but not GC B cells, are enriched for BLyS transcripts and co-localize with BLyS protein. This notion is further supported by our observation that the disparity in BLyS distribution within GCs is minimized in mixed BM chimeras where T cells cannot produce BLyS. The signals that regulate BLyS production by T FO lineage cells might involve co-stimulatory signals that regulate other effector functions, such as ICOS or PD-1/PD-L1 (Bauquet et al., 2009; Good-Jacobson et al., 2010). The nature of BLyS expressed by T FO cells is not yet clear. Given that the only known membrane isoform, delta BAFF, is not expressed in the T cell lineage (Gavin et al., 2005), local secretion of BLyS by T cells is a likely explanation of its restricted presence in the LZ.

Combined with prior findings, our results reveal distinct roles for systemic versus locally produced BLyS during the GC reaction, enabling GC initiation and maintenance versus affinity maturation, respectively. The severely reduced naive B cell numbers that accompany systemic BLyS deficiency probably underlie the premature GC termination and reduced class-switched antibody observed previously, because neither of these defects was observed in chimeras where only the T cell lineage lacks BLyS. This interpretation is consistent with the notion that incipient and ongoing GCs can be replenished from the naive pool (Schwickert et al., 2007), as well as recent studies showing that B cell antigen presentation is required for full T_{FH} differentiation (Goenka et al., 2011; Kerfoot et al., 2011), both of which predict impaired GC kinetics in B lymphopenic environments.

In contrast to systemic BLyS deficiency, local BLyS production is expendable for normal GC initiation, composition, and magnitude but appears critical for the survival of high affinity GC B cell clones generated by SHM. We favor this interpretation for several reasons. First, the reduced generation of high affinity, but not low affinity, ASCs and antibody reflects the absence of high affinity clones in the GC pool. Although BLyS can increase antibody secretion (Schneider et al., 1999), we consider this an unlikely mechanism for the selective decrease in the proportion of high affinity antibody because total NP-specific antibody concentrations were unchanged. Second, the presence of numerous mutations, including the W33L replacement mutation, indicates that SHM occurs; however, these GC B cells had acquired additional replacement mutations that reduced the strength of positive selection but did not abrogate the ability to bind antigen. It remains possible that the modestly reduced GC B cell numbers have an impact on high affinity antibody production in our mixed chimeras. However, the comparable output of class-switched ASCs and antibody, as well as the equivalent number of total R mutations among GC B cells in these mice and controls, argues in favor of altered selection rather than insufficient numbers of appropriately mutated cells. These possibilities are not mutually exclusive, and in either case posit a key role for T_{FH} cell–derived BLyS in the emergence or preservation of high affinity GC B cells.

Based on these findings, it is tempting to speculate that GC selection exploits the same relationship between BLyS availability and BCR signal strength that is active during transitional B cell selection, where increasing BCR signal strength imposes a greater need for survival signals via BR3. In the GC context, this would afford the deletion of all B cells experiencing strong BCR signals, such as those associated with the acquisition of self-reactivity. However, high affinity GC B cells that retain antigen specificity and hence antigen-presenting ability will be selectively spared, as they receive concentrated BLyS signals during cognate T_{FH} interactions. Indeed, high affinity B cells present more peptide than low-to-intermediate affinity B cells (Schwickert et al., 2011) and likely engage in longer cognate T_{FH} cell interactions, thus competing more effectively for BLyS. This model remains consistent with recent findings because some GC B cells maintain BCR signals (Khalil et al., 2012), and damped BCR signaling may be overcome by exceptionally high affinity. Alternatively, high affinity GC B cells may be more prone to death due to increased expression of pro-apoptotic mediators as a consequence of stronger BCR signals. This could also be balanced by the up-regulation of anti-apoptotic molecules by T_{FH} cell–derived BLyS. In either case, this general model resolves the seeming conundrum of simultaneous negative selection and affinity maturation within GCs because most B cells experiencing high affinity BCR engagement will be eliminated unless rescued by BLyS, and it predicts that events thwarting this mechanism could foster autoimmunity.

Downloaded from http://rupress.org/jem/article-pdf/211/1/45/1749587/jem_20130505.pdf by guest on 09 February 2026

MATERIALS AND METHODS

Mice and immunizations. Mice were maintained and used in accordance with the University of Pennsylvania Animal Care and Use Guidelines. University of Pennsylvania Institutional Animal Care and Use Committee approved all animal experiments. 8–14-wk-old C57BL/6J, TCR-β–deficient (B6.129P2-Tcrb^{tm1Mom}/J), SJL (*B6.SJL*-Ptprc^{a} Pepc^{b}/*Boy*), OTII transgenic females (B6.Cg-Tg(Tcr-αTcr-β) 425Cbn/J) were purchased from The Jackson Laboratory or NCI.TACI-deficient (von Bülow et al., 2001), IL21R-deficient (Ozaki et al., 2002), BLyS-deficient (Schiemann et al., 2001), and FoxP3-eGFP knockin (Lin et al., 2007) mice have been previously described. To generate mixed BM chimeras, BM from 8–12-wk-old TCR-β$^{-/-}$, BLyS$^{-/-}$, or WT mice was depleted of CD3^{+}, Gr1^{+}, and B220^{+} cells using MACS magnetic bead depletion (Miltenyi Biotec), and then mixed in a ratio of 25:75 TCR-β$^{-/-}$/BLyS$^{-/-}$ or 25:75 TCR-β$^{-/-}$/WT and injected i.v. into lethally irradiated (950 rads) WT mice. The mice were allowed to reconstitute for ≥11 wk. Mice were immunized i.p. with 50 μg NP-CGG or NP-OVA (Biosearch Technologies) with an NP conjugation ratio of 15 or 16 in alum.

BLyS detection. To detect bound BLyS on the surface of B cells, splenocytes incubated on ice were first labeled with rat anti–mouse BLyS antibody and subsequently labeled with PE-conjugated donkey anti–rat Ig (H+L) secondary antibody (Jackson ImmunoResearch Laboratories). The cells were washed and blocked with purified rat IgGs and then stained for other cell surface antigens. BLyS concentration in serum samples was determined by ELISA by Human Genome Sciences, Inc. (Scholz et al., 2008).

Immunohistochemistry. Spleens were immersed in O.C.T. (Tissue Tek), flash frozen using 2-methylbutane cooled with liquid nitrogen, and stored at −20°C. 7–8 μm sections were sliced in a cryostat (HM505E; Carl Zeiss), fixed with cold acetone, rehydrated in PBS, and incubated with antibodies in PBS containing 10% goat serum. Sections were stained with anti-BLyS antibody and then with donkey anti–rat antibody conjugated to FITC (described above), and then stained with PNA conjugated to Rhodamine (Vector Laboratories) or Alexa Fluor 647 (Invitrogen) and other cell surface antigens. Sections were mounted with Biomeda Gel/Mount mounting medium (Electron Microscopy Sciences). Images were obtained with using a Plan-Neofluar 25×/0.8 or Plan-Apochromat 63×/1.4 oil objective on a laser scanning confocal system (LSM510META NLO; Carl Zeiss) mounted on an inverted microscope (Axiovert 200M; version 4.0 LSM510 software; Carl Zeiss) at room temperature. Images were analyzed using ImageJ (version 1.46r; National Institutes of Health).

Flow cytometry. Antibodies or reagents reactive to the following antigens were used for flow cytometry: IgD (clone 11–26), CD4 (clone GK1.5), B220 (clone RA3-6B2), BR3 (clone 7H22-E16), CD62L (clone MEL-14), TCR-β (clone H57-597), and CD3ε (clone 145-2C11; eBioscience); F4/80 (clone BM8), Fas/CD95 (clone Jo2), CD19 (clone 1D3), Ly-6G/GR1 (clone RB6-8C5), CXCR5 (clone RF8B2), and CD35 (clone BC12; BD); Ig Lambda (SouthernBiotech); BLyS (clone 121808) and TACI (clone 166010; R&D Systems); PD1 (clone RMP1-30, BioLegend); and PNA-FITC (Vector Laboratories). NP was conjugated to APC in house. Exclusion of DAPI (Invitrogen) or TOPRO-3 (Invitrogen) was used to identify live cells and doublets were excluded by forward and side scatter height versus width analysis. Cells were analyzed on an LSRII cytometer or sorted on an Aria II (BD), and data were analyzed using FlowJo software (Tree Star).

In vitro B cell stimulations. CD23^{+} splenic B cells were enriched by positive selection using MACS bead system (Miltenyi Biotec) and were stimulated with F(ab)′$_2$ fragments of 10 μg/ml anti-IgM (Jackson ImmunoResearch Laboratories), 10 μg/ml anti-CD40 (clone HM40-3; BD), 100 ng/ml IL-21 (R&D Systems) for 3 d at 37°C and 5.5% CO_2 in RPMI/DMEM supplemented with 10% characterized FBS (HyClone), 1% Hepes (Gibco), 1% glutamine (Invitrogen), 50 μM 2-mercaptoethanol, 1% minimal essential amino acids (Gibco), and 1% OPI supplement (Sigma-Aldrich).

NP-specific ELISA/ELISpot. Immunosorb plates (Nunc) or Immobilon-P plates (Millipore) were coated with 10 μg/ml NP_4-BSA or NP_{33}-BSA (Biosearch Technologies) for ELISA or ELISPOT, respectively, and blocked with PBS containing 2% BSA. For ELISA, sera were incubated for 2 h at room temperature and plates developed with horseradish peroxidase–conjugated anti–mouse IgM or IgG1 antibodies (SouthernBiotech) using 3,3′, 5,5′ tetramethylbenzidine (TMB) substrate (BD). Color development was terminated with 2N H_2SO_4 then read on an EMax microplate reader (Molecular Devices). Purified anti-NP IgM or anti-NP IgG1 used as standards were a gift from G. Kelsoe (Duke University). For ELISPOTs, splenocyte suspensions were incubated for 4–5 h in RPMI/DMEM containing 10% FBS. Plates were developed with biotin-conjugated anti–mouse IgM or IgG1 antibodies (SouthernBiotech), followed by ExtrAvidin-Alkaline Phosphatase (Sigma-Aldrich) using NBT/BCIP substrate (Sigma-Aldrich), and color development was terminated with 1 M NaH_2PO_4. Spots were enumerated on CTL-ImmunoSpot reader (Cellular Technologies).

Quantitative PCR (qPCR) analysis. RNA was extracted with the RNeasy kit (QIAGEN) and reverse transcribed using SuperScript II Reverse transcription (Invitrogen) according to the manufacturer's protocols. cDNA was amplified using TaqMan Universal Master Mix (Applied Biosystems) and Taqman probes for various genes (Applied Biosystems). Real-time PCR was performed with an ABI 7300 (Applied Biosystems). Relative expression was calculated using 18S ribosomal subunit or GAPDH expression as an endogenous control for cells that were FACS sorted or stimulated in vitro, respectively.

SHM analysis. RNA was extracted from FACS-sorted NP^{+} GC B cells and reverse transcribed using RTCγ (Rohatgi et al., 2008) primers to enrich for IgG transcripts. cDNA was subjected to two rounds of nested PCR using Expand High Fidelity Polymerase (Roche) with 5′ primers for Vh186.2 (Lu et al., 2001) and 3′ primers for all Jh (Rohatgi et al., 2008). PCR cycling conditions were as follows: 95°C for 2.5 min, 52°C for 4 min, and 72°C for 2 min, followed by 40 cycles of 95°C for 1 min, 52°C for 1 min, 72°C for 1.5 min, and a final extension at 72°C for 5 min. Amplified bands of ∼350 bp were purified using PureLink gel extraction kit (Invitrogen) and cloned into pCR-TOPO vector using the TOPO TA Cloning kit (Invitrogen). Plasmid was prepared from individual bacterial colonies (GenElute HP Plasmid Miniprep kit; Sigma-Aldrich) and Vh inserts were sequenced at the Penn DNA Sequencing Facility.

All sequences were aligned to murine germline heavy chain Vh186.2 using IMGT database (Lefranc et al., 2005) and segregated into CDR and FWR (FWR1: 1–25; CDR1: 26–33; FWR2: 34–50; CDR2: 51–58; FWR3: 59–95; CDR3: 96–98). To determine if selection was occurring, we used the focused test, which compares the number of R mutations in the area of interest (CDR or FWR) to the total level of mutation in the whole Vh sequence (Hershberg et al., 2008; MacDonald et al., 2010; Uduman et al., 2011). The actual level of S mutations and germline sequence are together used to calculate an expected relative level of R mutations. If the observed level of R mutations is significantly greater or lower than expected, this is an indication of positive selection or negative selection, respectively. As we and others have demonstrated, the analysis of mutations from groups of sequences enhances sensitivity of detection without sacrificing accuracy, thus considering the force of selection on the set of sequences rather than individually.

To relate different sequences from the same experiment, which individually could have different numbers of mutations, we measured selection strength. We converted the observed level of mutation and expected level of mutation to the log odds ratio of the two; higher values indicate more positive selection and vice versa. We quantified selection strength using the BASELINe algorithm available on the web. This algorithm extrapolates from the mutation pattern the distribution of potential selection pressure values that could produce it (Uduman et al., 2011; Yaari et al., 2012). This method analyzes all mutations collected from the same experimental condition and takes into account mutations that came from the same sequences and/or clones, and whether they occur in CDR or FWR. It creates a probability distribution function of the estimated selection strength from which these

Downloaded from http://rupress.org/jem/article-pdf/211/1/45/1749587/jem_20130505.pdf by guest on 09 February 2026

mutations could arise in those positions. Information about the certainty of the estimated values and the consistency of selection pressures across all sequences analyzed is reflected in the width of the distribution: the narrower the distribution, the more precise is the assessment of selection strength (positive or negative) from the pattern of mutations observed. In this fashion, BASELINe is capable of comparing experiments with unequal sequence numbers, where the calculated distribution of selection strength may not be as narrow.

Statistical analysis. Data (other than for SHM analyses) were tested for statistical significance at $\alpha = 0.05$ in a two-tailed Student's *t* test.

We thank Xinyu Zhao of the University of Pennsylvania Cell and Developmental Microscopy Core for assistance with microscopy. We thank Drs. Avinash Bhandoola and Patrick Guirnalda for helpful discussion and critical review of the manuscript, and Ms. Laurie Baker for assistance in manuscript preparation.

This work was funded by grants AI073939 (National Institutes of Health [NIH]) and a Sponsored Research Agreement (Human Genome Sciences, Inc.) to M.P. Cancro, and grant AR050193 (NIH) to W. Stohl. W.J. Leonard is supported by the Division of Intramural Research, National Heart, Lung, and Blood Institute, NIH.

The authors have no competing financial interests.

Submitted: 11 March 2013
Accepted: 26 November 2013

REFERENCES

Allen, C.D., and J.G. Cyster. 2008. Follicular dendritic cell networks of primary follicles and germinal centers: phenotype and function. *Semin. Immunol.* 20:14–25. http://dx.doi.org/10.1016/j.smim.2007.12.001

Bauquet, A.T., H. Jin, A.M. Paterson, M. Mitsdoerffer, I.C. Ho, A.H. Sharpe, and V.K. Kuchroo. 2009. The costimulatory molecule ICOS regulates the expression of c-Maf and IL-21 in the development of follicular T helper cells and TH-17 cells. *Nat. Immunol.* 10:167–175. http://dx.doi.org/10.1038/ni.1690

Bossen, C., T.G. Cachero, A. Tardivel, K. Ingold, L. Willen, M. Dobles, M.L. Scott, A. Maquelin, E. Belnoue, C.A. Siegrist, et al. 2008. TACI, unlike BAFF-R, is solely activated by oligomeric BAFF and APRIL to support survival of activated B cells and plasmablasts. *Blood.* 111:1004–1012. http://dx.doi.org/10.1182/blood-2007-09-110874

Cancro, M.P. 2004. Peripheral B-cell maturation: the intersection of selection and homeostasis. *Immunol. Rev.* 197:89–101. http://dx.doi.org/10.1111/j.0105-2896.2004.0099.x

Chung, Y., S. Tanaka, F. Chu, R.I. Nurieva, G.J. Martinez, S. Rawal, Y.H. Wang, H. Lim, J.M. Reynolds, X.H. Zhou, et al. 2011. Follicular regulatory T cells expressing Foxp3 and Bcl-6 suppress germinal center reactions. *Nat. Med.* 17:983–988. http://dx.doi.org/10.1038/nm.2426

Foy, T.M., D.M. Shepherd, F.H. Durie, A. Aruffo, J.A. Ledbetter, and R.J. Noelle. 1993. In vivo CD40-gp39 interactions are essential for thymus-dependent humoral immunity. II. Prolonged suppression of the humoral immune response by an antibody to the ligand for CD40, gp39. *J. Exp. Med.* 178:1567–1575. http://dx.doi.org/10.1084/jem.178.5.1567

Gavin, A.L., B. Duong, P. Skog, D. Aït-Azzouzene, D.R. Greaves, M.L. Scott, and D. Nemazee. 2005. deltaBAFF, a splice isoform of BAFF, opposes full-length BAFF activity in vivo in transgenic mouse models. *J. Immunol.* 175:319–328.

Goenka, R., L.G. Barnett, J.S. Silver, P.J. O'Neill, C.A. Hunter, M.P. Cancro, and T.M. Laufer. 2011. Cutting edge: dendritic cell-restricted antigen presentation initiates the follicular helper T cell program but cannot complete ultimate effector differentiation. *J. Immunol.* 187:1091–1095. http://dx.doi.org/10.4049/jimmunol.1100853

Good-Jacobson, K.L., C.G. Szumilas, L. Chen, A.H. Sharpe, M.M. Tomayko, and M.J. Shlomchik. 2010. PD-1 regulates germinal center B cell survival and the formation and affinity of long-lived plasma cells. *Nat. Immunol.* 11:535–542. http://dx.doi.org/10.1038/ni.1877

Gorelik, L., K. Gilbride, M. Dobles, S.L. Kalled, D. Zandman, and M.L. Scott. 2003. Normal B cell homeostasis requires B cell activation factor production by radiation-resistant cells. *J. Exp. Med.* 198:937–945. http://dx.doi.org/10.1084/jem.20030789

Grouard, G., I. Durand, L. Filgueira, J. Banchereau, and Y.J. Liu. 1996. Dendritic cells capable of stimulating T cells in germinal centres. *Nature.* 384:364–367. http://dx.doi.org/10.1038/384364a0

Han, S., K. Hathcock, B. Zheng, T.B. Kepler, R. Hodes, and G. Kelsoe. 1995. Cellular interaction in germinal centers. Roles of CD40 ligand and B7-2 in established germinal centers. *J. Immunol.* 155:556–567.

Hao, Z., G.S. Duncan, J. Seagal, Y.W. Su, C. Hong, J. Haight, N.J. Chen, A. Elia, A. Wakeham, W.Y. Li, et al. 2008. Fas receptor expression in germinal-center B cells is essential for T and B lymphocyte homeostasis. *Immunity.* 29:615–627. http://dx.doi.org/10.1016/j.immuni.2008.07.016

Hase, H., Y. Kanno, M. Kojima, K. Hasegawa, D. Sakurai, H. Kojima, N. Tsuchiya, K. Tokunaga, N. Masawa, M. Azuma, et al. 2004. BAFF/BLyS can potentiate B-cell selection with the B-cell coreceptor complex. *Blood.* 103:2257–2265. http://dx.doi.org/10.1182/blood-2003-08-2694

Hershberg, U., M. Uduman, M.J. Shlomchik, and S.H. Kleinstein. 2008. Improved methods for detecting selection by mutation analysis of Ig V region sequences. *Int. Immunol.* 20:683–694. http://dx.doi.org/10.1093/intimm/dxn026

Hsu, B.L., S.M. Harless, R.C. Lindsley, D.M. Hilbert, and M.P. Cancro. 2002. Cutting edge: BLyS enables survival of transitional and mature B cells through distinct mediators. *J. Immunol.* 168:5993–5996.

Huntington, N.D., Y. Xu, H. Puthalakath, A. Light, S.N. Willis, A. Strasser, and D.M. Tarlinton. 2006. CD45 links the B cell receptor with cell survival and is required for the persistence of germinal centers. *Nat. Immunol.* 7:190–198. http://dx.doi.org/10.1038/ni1292

Johnston, R.J., A.C. Poholek, D. DiToro, I. Yusuf, D. Eto, B. Barnett, A.L. Dent, J. Craft, and S. Crotty. 2009. Bcl6 and Blimp-1 are reciprocal and antagonistic regulators of T follicular helper cell differentiation. *Science.* 325:1006–1010. http://dx.doi.org/10.1126/science.1175870

Kapasi, Z.F., D. Qin, W.G. Kerr, M.H. Kosco-Vilbois, L.D. Shultz, J.G. Tew, and A.K. Szakal. 1998. Follicular dendritic cell (FDC) precursors in primary lymphoid tissues. *J. Immunol.* 160:1078–1084.

Kerfoot, S.M., G. Yaari, J.R. Patel, K.L. Johnson, D.G. Gonzalez, S.H. Kleinstein, and A.M. Haberman. 2011. Germinal center B cell and T follicular helper cell development initiates in the interfollicular zone. *Immunity.* 34:947–960. http://dx.doi.org/10.1016/j.immuni.2011.03.024

Khalil, A.M., J.C. Cambier, and M.J. Shlomchik. 2012. B cell receptor signal transduction in the GC is short-circuited by high phosphatase activity. *Science.* 336:1178–1181. http://dx.doi.org/10.1126/science.1213368

Krautler, N.J., V. Kana, J. Kranich, Y. Tian, D. Perera, D. Lemm, P. Schwarz, A. Armulik, J.L. Browning, M. Tallquist, et al. 2012. Follicular dendritic cells emerge from ubiquitous perivascular precursors. *Cell.* 150:194–206. http://dx.doi.org/10.1016/j.cell.2012.05.032

Lefranc, M.P., V. Giudicelli, Q. Kaas, E. Duprat, J. Jabado-Michaloud, D. Scaviner, C. Ginestoux, O. Clément, D. Chaume, and G. Lefranc. 2005. IMGT, the international ImMunoGeneTics information system. *Nucleic Acids Res.* 33:D593–D597. http://dx.doi.org/10.1093/nar/gki065

Lesley, R., Y. Xu, S.L. Kalled, D.M. Hess, S.R. Schwab, H.B. Shu, and J.G. Cyster. 2004. Reduced competitiveness of autoantigen-engaged B cells due to increased dependence on BAFF. *Immunity.* 20:441–453. http://dx.doi.org/10.1016/S1074-7613(04)00079-2

Lin, W., D. Haribhai, L.M. Relland, N. Truong, M.R. Carlson, C.B. Williams, and T.A. Chatila. 2007. Regulatory T cell development in the absence of functional Foxp3. *Nat. Immunol.* 8:359–368. http://dx.doi.org/10.1038/ni1445

Linterman, M.A., L. Beaton, D. Yu, R.R. Ramiscal, M. Srivastava, J.J. Hogan, N.K. Verma, M.J. Smyth, R.J. Rigby, and C.G. Vinuesa. 2010. IL-21 acts directly on B cells to regulate Bcl-6 expression and germinal center responses. *J. Exp. Med.* 207:353–363. http://dx.doi.org/10.1084/jem.20091738

Linterman, M.A., W. Pierson, S.K. Lee, A. Kallies, S. Kawamoto, T.F. Rayner, M. Srivastava, D.P. Divekar, L. Beaton, J.J. Hogan, et al. 2011. Foxp3+ follicular regulatory T cells control the germinal center response. *Nat. Med.* 17:975–982. http://dx.doi.org/10.1038/nm.2425

Lu, Y.F., M. Singh, and J. Cerny. 2001. Canonical germinal center B cells may not dominate the memory response to antigenic challenge. *Int. Immunol.* 13:643–655. http://dx.doi.org/10.1093/intimm/13.5.643

Downloaded from http://rupress.org/jem/article-pdf/211/1/45/1749587/jem_20130505.pdf by guest on 09 February 2026

MacDonald, C.M., L. Boursier, D.P. D'Cruz, D.K. Dunn-Walters, and J. Spencer. 2010. Mathematical analysis of antigen selection in somatically mutated immunoglobulin genes associated with autoimmunity. *Lupus*. 19:1161–1170. http://dx.doi.org/10.1177/0961203310367657

Mackay, F., and P. Schneider. 2009. Cracking the BAFF code. *Nat. Rev. Immunol.* 9:491–502. http://dx.doi.org/10.1038/nri2572

Mantchev, G.T., C.S. Cortesão, M. Rebrovich, M. Cascalho, and R.J. Bram. 2007. TACI is required for efficient plasma cell differentiation in response to T-independent type 2 antigens. *J. Immunol.* 179:2282–2288.

McHeyzer-Williams, L.J., N. Pelletier, L. Mark, N. Fazilleau, and M.G. McHeyzer-Williams. 2009. Follicular helper T cells as cognate regulators of B cell immunity. *Curr. Opin. Immunol.* 21:266–273. http://dx.doi.org/10.1016/j.coi.2009.05.010

Moore, P.A., O. Belvedere, A. Orr, K. Pieri, D.W. LaFleur, P. Feng, D. Soppet, M. Charters, R. Gentz, D. Parmelee, et al. 1999. BLyS: member of the tumor necrosis factor family and B lymphocyte stimulator. *Science*. 285:260–263. http://dx.doi.org/10.1126/science.285.5425.260

O'Connor, B.P., V.S. Raman, L.D. Erickson, W.J. Cook, L.K. Weaver, C. Ahonen, L.L. Lin, G.T. Mantchev, R.J. Bram, and R.J. Noelle. 2004. BCMA is essential for the survival of long-lived bone marrow plasma cells. *J. Exp. Med.* 199:91–98. http://dx.doi.org/10.1084/jem.20031330

Ozaki, K., R. Spolski, C.G. Feng, C.F. Qi, J. Cheng, A. Sher, H.C. Morse III, C. Liu, P.L. Schwartzberg, and W.J. Leonard. 2002. A critical role for IL-21 in regulating immunoglobulin production. *Science*. 298:1630–1634. http://dx.doi.org/10.1126/science.1077002

Rahman, Z.S., S.P. Rao, S.L. Kalled, and T. Manser. 2003. Normal induction but attenuated progression of germinal center responses in BAFF and BAFF-R signaling-deficient mice. *J. Exp. Med.* 198:1157–1169. http://dx.doi.org/10.1084/jem.20030495

Rohatgi, S., P. Ganju, and D. Sehgal. 2008. Systematic design and testing of nested (RT-)PCR primers for specific amplification of mouse rearranged/expressed immunoglobulin variable region genes from small number of B cells. *J. Immunol. Methods*. 339:205–219. http://dx.doi.org/10.1016/j.jim.2008.09.017

Sage, P.T., L.M. Francisco, C.V. Carman, and A.H. Sharpe. 2013. The receptor PD-1 controls follicular regulatory T cells in the lymph nodes and blood. *Nat. Immunol.* 14:152–161. http://dx.doi.org/10.1038/ni.2496

Schiemann, B., J.L. Gommerman, K. Vora, T.G. Cachero, S. Shulga-Morskaya, M. Dobles, E. Frew, and M.L. Scott. 2001. An essential role for BAFF in the normal development of B cells through a BCMA-independent pathway. *Science*. 293:2111–2114. http://dx.doi.org/10.1126/science.1061964

Schneider, P., F. MacKay, V. Steiner, K. Hofmann, J.L. Bodmer, N. Holler, C. Ambrose, P. Lawton, S. Bixler, H. Acha-Orbea, et al. 1999. BAFF, a novel ligand of the tumor necrosis factor family, stimulates B cell growth. *J. Exp. Med.* 189:1747–1756. http://dx.doi.org/10.1084/jem.189.11.1747

Scholz, J.L., J.E. Crowley, M.M. Tomayko, N. Steinel, P.J. O'Neill, W.J. Quinn III, R. Goenka, J.P. Miller, Y.H. Cho, V. Long, et al. 2008. BLyS inhibition eliminates primary B cells but leaves natural and acquired humoral immunity intact. *Proc. Natl. Acad. Sci. USA*. 105:15517–15522. http://dx.doi.org/10.1073/pnas.0807841105

Schwickert, T.A., R.L. Lindquist, G. Shakhar, G. Livshits, D. Skokos, M.H. Kosco-Vilbois, M.L. Dustin, and M.C. Nussenzweig. 2007. In vivo imaging of germinal centres reveals a dynamic open structure. *Nature*. 446:83–87. http://dx.doi.org/10.1038/nature05573

Schwickert, T.A., G.D. Victora, D.R. Fooksman, A.O. Kamphorst, M.R. Mugnier, A.D. Gitlin, M.L. Dustin, and M.C. Nussenzweig. 2011. A dynamic T cell-limited checkpoint regulates affinity-dependent B cell entry into the germinal center. *J. Exp. Med.* 208:1243–1252. http://dx.doi.org/10.1084/jem.20102477

Seshasayee, D., P. Valdez, M. Yan, V.M. Dixit, D. Tumas, and I.S. Grewal. 2003. Loss of TACI causes fatal lymphoproliferation and autoimmunity, establishing TACI as an inhibitory BLyS receptor. *Immunity*. 18:279–288. http://dx.doi.org/10.1016/S1074-7613(03)00025-6

Shaffer, A.L., K.I. Lin, T.C. Kuo, X. Yu, E.M. Hurt, A. Rosenwald, J.M. Giltnane, L. Yang, H. Zhao, K. Calame, and L.M. Staudt. 2002. Blimp-1 orchestrates plasma cell differentiation by extinguishing the mature B cell gene expression program. *Immunity*. 17:51–62. http://dx.doi.org/10.1016/S1074-7613(02)00335-7

Stadanlick, J.E., M. Kaileh, F.G. Karnell, J.L. Scholz, J.P. Miller, W.J. Quinn III, R.J. Brezski, L.S. Treml, K.A. Jordan, J.G. Monroe, et al. 2008. Tonic B cell antigen receptor signals supply an NF-kappaB substrate for prosurvival BLyS signaling. *Nat. Immunol.* 9:1379–1387. http://dx.doi.org/10.1038/ni.1666

Thompson, J.S., S.A. Bixler, F. Qian, K. Vora, M.L. Scott, T.G. Cachero, C. Hession, P. Schneider, I.D. Sizing, C. Mullen, et al. 2001. BAFF-R, a newly identified TNF receptor that specifically interacts with BAFF. *Science*. 293:2108–2111. http://dx.doi.org/10.1126/science.1061965

Tsuji, S., C. Cortesão, R.J. Bram, J.L. Platt, and M. Cascalho. 2011. TACI deficiency impairs sustained Blimp-1 expression in B cells decreasing long-lived plasma cells in the bone marrow. *Blood*. 118:5832–5839. http://dx.doi.org/10.1182/blood-2011-05-353961

Uduman, M., G. Yaari, U. Hershberg, J.A. Stern, M.J. Shlomchik, and S.H. Kleinstein. 2011. Detecting selection in immunoglobulin sequences. *Nucleic Acids Res.* 39(suppl):W499–W504. http://dx.doi.org/10.1093/nar/gkr413

Victora, G.D., and M.C. Nussenzweig. 2012. Germinal centers. *Annu. Rev. Immunol.* 30:429–457. http://dx.doi.org/10.1146/annurev-immunol-020711-075032

Victora, G.D., T.A. Schwickert, D.R. Fooksman, A.O. Kamphorst, M. Meyer-Hermann, M.L. Dustin, and M.C. Nussenzweig. 2010. Germinal center dynamics revealed by multiphoton microscopy with a photoactivatable fluorescent reporter. *Cell*. 143:592–605. http://dx.doi.org/10.1016/j.cell.2010.10.032

von Bülow, G.U., and R.J. Bram. 1997. NF-AT activation induced by a CAML-interacting member of the tumor necrosis factor receptor superfamily. *Science*. 278:138–141. http://dx.doi.org/10.1126/science.278.5335.138

von Bülow, G.U., J.M. van Deursen, and R.J. Bram. 2001. Regulation of the T-independent humoral response by TACI. *Immunity*. 14:573–582. http://dx.doi.org/10.1016/S1074-7613(01)00130-3

Wang, Y., and R.H. Carter. 2005. CD19 regulates B cell maturation, proliferation, and positive selection in the FDC zone of murine splenic germinal centers. *Immunity*. 22:749–761. http://dx.doi.org/10.1016/j.immuni.2005.04.012

Yaari, G., M. Uduman, and S.H. Kleinstein. 2012. Quantifying selection in high-throughput Immunoglobulin sequencing data sets. *Nucleic Acids Res.* 40:e134. http://dx.doi.org/10.1093/nar/gks457

Yan, M., J.R. Brady, B. Chan, W.P. Lee, B. Hsu, S. Harless, M. Cancro, I.S. Grewal, and V.M. Dixit. 2001a. Identification of a novel receptor for B lymphocyte stimulator that is mutated in a mouse strain with severe B cell deficiency. *Curr. Biol.* 11:1547–1552. http://dx.doi.org/10.1016/S0960-9822(01)00481-X

Yan, M., H. Wang, B. Chan, M. Roose-Girma, S. Erickson, T. Baker, D. Tumas, I.S. Grewal, and V.M. Dixit. 2001b. Activation and accumulation of B cells in TACI-deficient mice. *Nat. Immunol.* 2:638–643. http://dx.doi.org/10.1038/89790

Zotos, D., J.M. Coquet, Y. Zhang, A. Light, K. D'Costa, A. Kallies, L.M. Corcoran, D.I. Godfrey, K.M. Toellner, M.J. Smyth, et al. 2010. IL-21 regulates germinal center B cell differentiation and proliferation through a B cell-intrinsic mechanism. *J. Exp. Med.* 207:365–378. http://dx.doi.org/10.1084/jem.20091777

Downloaded from http://rupress.org/jem/article-pdf/211/1/45/1749587/jem_20130505.pdf by guest on 09 February 2026